Accelerated retrofit of bridge columns using UHPC shell – Phase I: Feasibility Study

Quarterly Progress Report

For the period ending June 30, 2018

Submitted by

Atorod Azizinamini

Graduate students

Mahsa Farzad

Affiliation: Civil & Environmental Engineering Department

Florida International University

ACCELERATED BRIDGE CONSTRUCTION
UNIVERSITY TRANSPORTATION CENTER

Submitted to:

ABC-UTC

Florida International University

Miami, FL

1 Introduction

The degradation rate of marine piles is affected by a variety of factors such as cracking and spalling of concrete due to the harsh environment, loss of reinforcement, and lack of confinement in concrete due to corrosion As a result, the structural integrity and load-carrying capacity, unusually columnar supporting of such structures, will reduce drastically.

Such undesired phenomenon requires the development of new techniques and materials to restore the deficient structure in a timely manner. The rehabilitation process should increase the service level and achieve a longer life expectancy of the structure.

The typical repair strategies are concrete jacketing, steel jacketing, and FRP wrapping [1]–[6]. Concrete jacketing, the most conventional repair method, is quite capable of providing the necessary strength, stiffness, and ductility [7]–[12]. However, it increases the cross-sectional dimensions and the dead weight of the structure, which could significantly alter the dynamic characteristics of the system. Besides, restoring the structure through concrete jacketing creates concrete overlay layers, which induces additional stresses and results in cracking of the new layer and de-bonding [9], [13], [14].

The advent of new concrete compounds, such as UHPC, provides the potential to improve both durability and resistance of the retrofitted structure. UHPC offers superior mechanical properties such as high chemical resistance, low fatigue loss, high flexibility, high tensile strength, high impermeability, and high energy absorption [15]–[23]. Therefore, UHPC as a strengthening compound in structures has received considerable attention [13], [24]–[28]

Farhat et al. tested strengthened beams via UHPC strips. They used an epoxy adhesive to bond UHPC and the substrate concrete, and the results showed that UHPC could prevent shear failure of the beams and increase the failure load up to 86% [24]. Beschi et al. investigated the application of UHPC for the repair and strengthening of beam-column joints, and the findings indicated a remarkable increased bearing capacity [26]. Habel et al. examined the combination of UHPC with reinforcing steel bars to rehabilitate the existing concrete elements. The results showed that UHPC strengthens the existing structures and increases their ultimate moment capacity [13]. The flexural strength and the ductility of UHPC are profoundly affected by steel fiber percentage. Studies show that although fibers' orientation and distribution has a negligible effect on the pre-cracking behavior, it noticeably changes the post-cracking phase [29].

The properties of UHPC make it a suitable choice as the repair material for retrofitting the damaged body of the marine piles, and application of UHPC could provide an efficient solution to address the pressing issue of bridge rehabilitation [30]. However, there have been very limited studies investigating the feasibility of using this material to repair concrete columns.

This research aims to investigate the performance of UHPC as retrofit material for damaged bridge columns. To achieve this goal, an experimental study was designed to evaluate the mechanical performance of the repaired columns under a combination of static axial and cyclic lateral loads (to simulate operational conditions).

In the rest of this article, Section 2 explains the column construction, artificial damage and repair, test setup, and instrumentation procedures; Section 3 outlines test observations and results; and Section 5 presents the concluding remarks.

2 Research Approach

To evaluate the performance of UHPC as repair material, column prototypes were designed and built to represent a bridge pier or a building column. The columns were then artificially damaged and repaired with UHPC. The specimens were scaled as 1/4 of a bridge column with a height to diameter ratio of 5, and their stubs represented a discontinuity, such as a beam column joint or a footing. The dimensions of the test columns are presented in Figure 1.

The first phase of the repair procedure is the mechanical removal of the damaged concrete cover and cleaning the substrate from residue particles and creation of exposed aggregate which is essential to have a good bond between UHPC and existing concrete in repaired areas. Then the lost, corroded, or extremely deformed reinforcement is cut and replaced. Before casting UHPC, the substrate concrete surface is saturated with water. At the end, all the cavities are filled with UHPC using proper forming.

The flowability of UHPC makes it possible to fill different shapes of cavities, and its low permeability acts as a barrier to environmental intrusions. UHPC has a relatively early strength gain, which reduces the traffic interruptions, and its durability decreases the life-cycle cost of the repair.

2.1 Experiment Design

In this research, three Reinforced Concrete (RC) columns were cast and artificially damaged with spalling cover. Two of the damaged columns were repaired with UHPC, and one column, with no repair, was used as the test baseline.

Furthermore, to investigate the amount of confinement provided by UHPC in the damaged zone, one of the repaired columns included confining reinforcement and the other one was strengthened using only UHPC. The column portion of the test specimens was embedded in a heavily reinforced base, forming the support condition for the columns during the test.

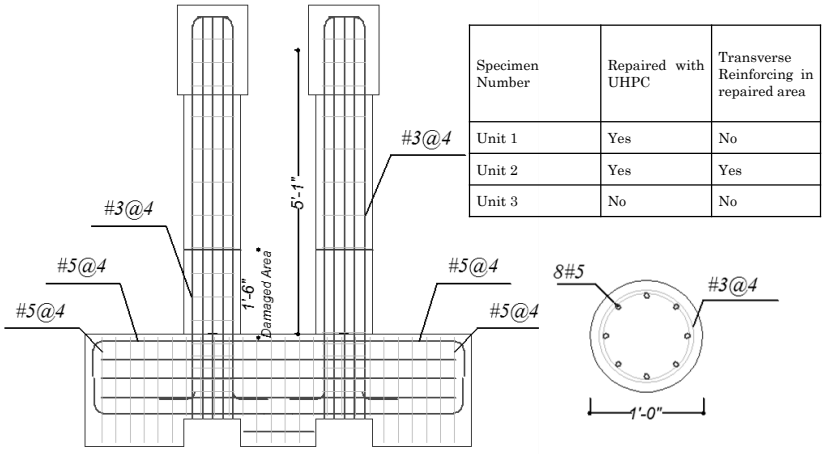

Specimen Number	Repaired with UHPC	Transverse Reinforcing in repaired area
Unit 1	Yes	No
Unit 2	Yes	Yes
Unit 3	No	No

Figure 1. Test specimen dimensions.

2.2 Test Specimen Construction

The columns were longitudinally reinforced with eight Grade 60 ksi (414 MPa), #5 (MM16) steel bars, resulting in 2.2% longitudinal steel reinforcement ratios (ρ=2.2%). All columns were initially equipped with 0.375 in. (10 mm) diameter steel hoops with 4 in. (10 cm) spacing

on center, in accordance with AASHTO specification for the non-seismic area [31]. The construction process of a typical specimen formwork, caging and casting is shown in Figure 2.

Figure 2. The construction process of a typical specimen: a) formwork and caging, b) simulating the damage, c) erecting the columns, and d) casting the concrete substrate.

The artificial damages were created similar to partial concrete spalling, and they were made in the lower portion of the columns to achieve flexural enhancement. To create artificial damage, the bottom 18 in. (460 mm) of each column was filled with cream insulating foam (see Figure 2b) according to the section view presented in Figure 3.

Specimens were cast and stripped after seven days. The curing regime used for this study was moist curing using plastic sheets for seven more days and air-dried allowing the specimens to remain in an ambient laboratory environment until repair.

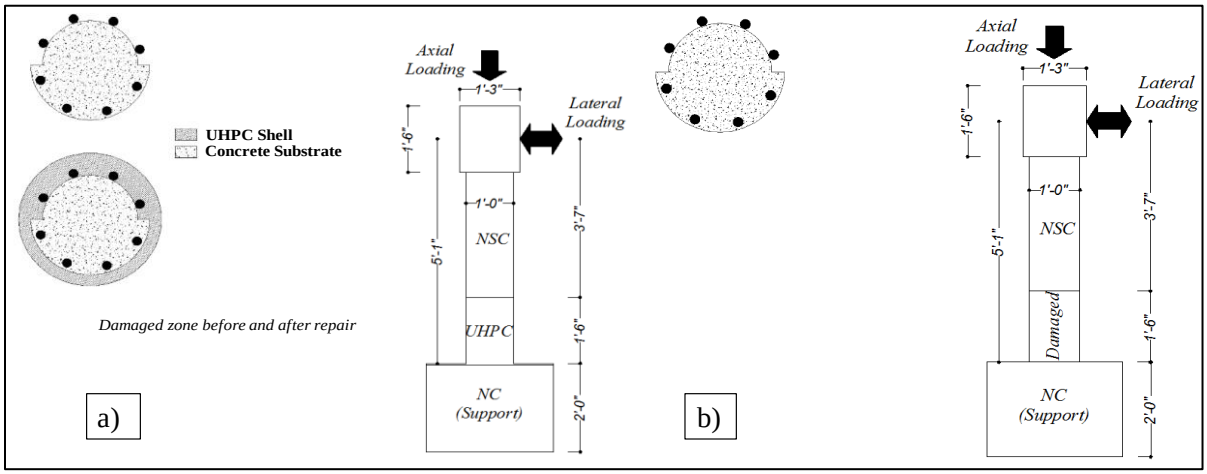

Figure 3. Damaged part before and after repair using UHPFRC shell (Unit 1 and 2), b) Damaged part with no repair (Unit 3)

2.3 Repair Procedure

The areas of the test specimens including damage were sandblasted to expose the aggregate and clean the substrate from residue particles. The cleaned surface was sprayed with water and allowed to dry to reach dry-surface condition. The damaged area was cast with UHPC. The UHPC used in this study was an available commercial product, Ductal®, made by Lafarge, and composed of premix powder, water, superplasticizer, and 2% metallic fibers by

volume. The fibers were 0.4 in. (10 mm) long, with a tensile strength of 406 ksi (2800 MPa). The repair procedure is presented in Figure 4.

All repaired specimens were de-molded after 24 hours. Each specimen was then covered in plastic to prevent drying out and kept at laboratory temperature for seven days. The specimens remained in a standard laboratory environment until testing.

Figure 4. Repair Procedure: a) damaged part before repair, b) damaged part after sandblasting treatment, c) formwork for the repair plastering, d) casting UHPC, and e) damaged part after repair.

2.4 Material Properties

The workability of the prepared UHPC mixture was measured in accordance with Precast/Pre-stressed Concrete Institute (PCI) guidelines [32] and ASTM C1437 [33]. The compressive test was carried out on cylinder specimens of 3 in. (76 mm) diameter and six in. tall (152 mm) using ASTM C 39 guideline [34]. Fifteen cylinders were tested to determine the compressive strength at the age of 3, 7, 14, 28, and 60 days of curing (3 cylinders each). Furthermore, the tensile properties of UHPC were obtained through the flexural toughness test procedure presented in ASTM C1018 [35]. Three small-scale test samples (20×6×6) inches (51×15×15 cm) with a span of 18 inches (46 cm) were cast and tested after 28 days. Results are presented in Table 1.

Table 1. Properties of UHPC

Workability Test Parameter		
Slump Flow Test		34.0 in. (86 cm)
J-ring Test		32.5 in. (83 cm)
Static Flowability		8 in. (20 cm)
Dynamic Flowability		10 in. (25 cm)
Hardened properties test		
Age	Compressive strength	Modulus of rupture
3	10.0 ksi (69 MPa)	-
7	10.9 ksi (75 MPa)	-
14	16.1 ksi (111 MPa)	-
28	25.2 ksi (174 MPa)	3.2 ksi (36 MPa)
60	28.0 ksi (193 MPa)	-

Local ready-mix normal density concrete was used to cast substrate concrete in layers and vibrated thoroughly. The concrete mix had an aggregate cement weight ratio of 5.8, water-cement ratio of 0.45, and a maximum aggregate of 1 in. (25 mm). The compression and tensile properties of the substrate concrete were obtained by testing three 4×8 in. (10×20 cm) cylindrical specimens, after 28 and 60 days of curing. Results of workability, compression,

and tension tests are presented in Table 2. Table 3 presents the mechanical properties of the steel bars used in this study.

Table 2. Properties of Substrate Concrete

Workability Test Parameter		
Slump	5 in. (13 cm)	
Hardened properties test		
Age (days)	Compressive strength	Modulus of rupture
28	7.0 ksi (48 MPa)	0.8 ksi (5.5 MPa)
60	7.2 ksi (50 MPa)	-

Table 3. Reinforcing Steel Properties

Bar size	**fy**	**fu**	**Elongation**
#5	68.6 ksi (473 MPa)	113 ksi (779 MPa)	12%
#3	71.8 ksi (495 MPa)	111 ksi (765 MPa)	13%

2.5 Test Setup and Instrumentation

Specimens were set up and aligned in a vertical position, and the footings were tied down to avoid any rotation. The dead load was simulated by applying an external post-tensioning force equal to 0.1 $f'_c A_g$ (56 kips), where f'_c is the compressive strength of the 28-day-old concrete substrate, and A_g is the gross cross-sectional area of the column. Test specimens were first subjected to constant axial load and then cyclic lateral loads at increasing displacement levels. A typical test specimen, with loading devices attached, is shown in Figure 5.

Figure 5. Test setup.

Each column was laterally loaded for three cycles at each displacement ductility ratio. The displacement ductility ratio μ_Δ is defined as the ratio of peak lateral displacement to the first yield displacement. The first yield displacement, Δ_y, is determined during the first loading cycle of each test. Its value was defined as the displacement corresponding to the point where initial and final tangents to the load-deflection curve meet, as shown in Figure 6.

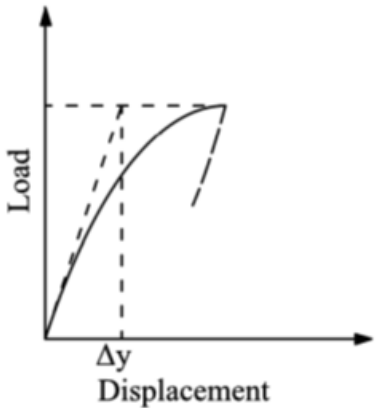

Figure 6. Experimental definition of first yield displacement.

Test specimens were instrumented to allow measuring curvature distribution along the height of the column, and lateral load vs. lateral displacement response of the test specimens. The column and footing surface was painted white to facilitate monitoring the crack pattern formation, during the tests. The combined cyclic lateral load and constant axial load were applied up to the point of failure. Deflections and applied loads were monitored continuously and crack development of the column were traced and recorded, at the peak of each displacement ductility ratio.

3 Test Observations

All test specimens failed by buckling and fracture of longitudinal steels, coinciding with a sharp drop in lateral load carrying capacity of the columns. The most extensive damage was concentrated between 4 and 18 in. (10-45 cm), 3 and 22 in. (8-56 cm), and 0.5 to 18 in. (1.2-46 cm) from the face of the stub, for test specimens 1 to 3, respectively. Figure 7 through Figure 9 shows the condition of the test specimens at different displacement ductility ratios.

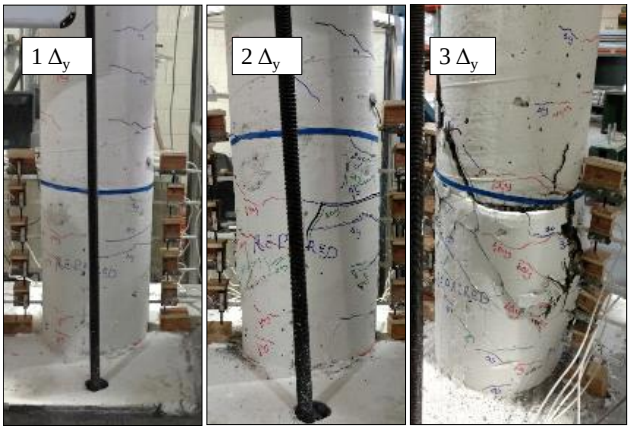

Figure 7. Test specimen at the end of each loading cycle (Unit 1).

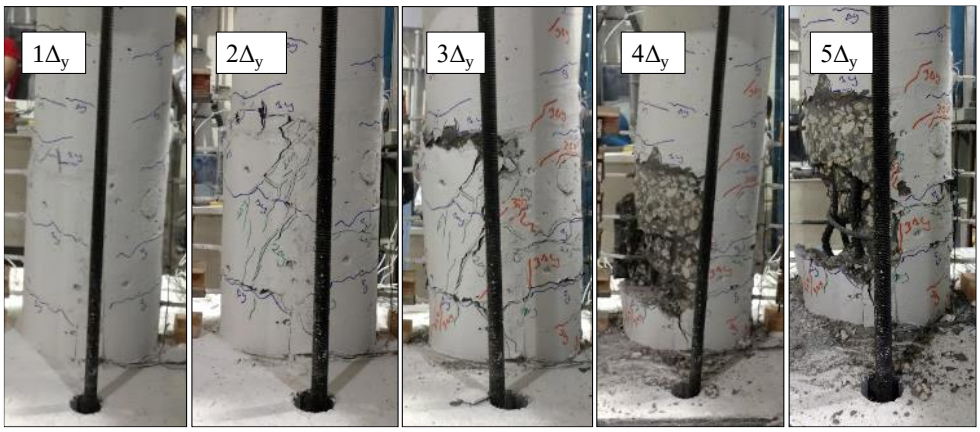

Figure 8. Test specimen at the end of each loading cycle (Unit 2).

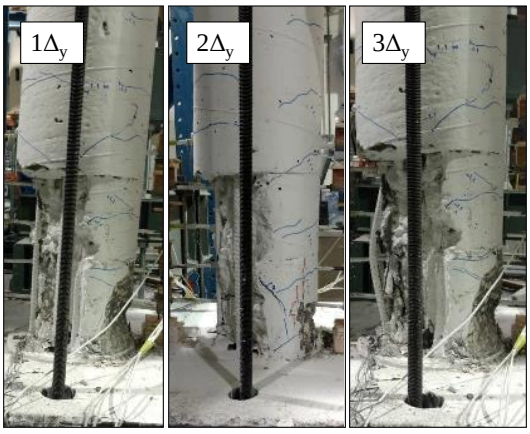

Figure 9. Test specimen at the end of each loading cycle (Unit 3).

Figure 10 indicates good bonding between substrate concrete and UHPC, as failure surface is located outside of interface between two concrete layers and in the normal strength concrete. Lack of any delamination across the circumferential shell of UHPC shows the effectiveness of the surface preparation, which is a prerequisite for a successful restoration.

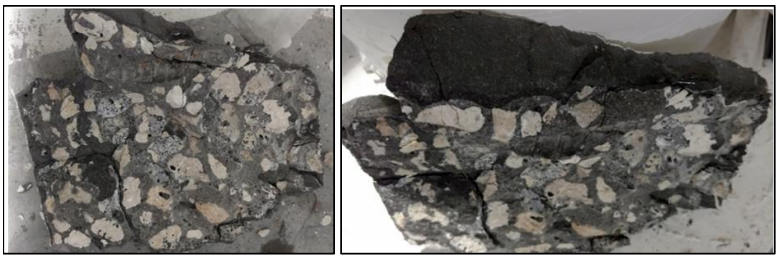
Figure 10. Bond between concrete substrate and UHPC in the repair zone.

During testing Unit 1 (specimen without stirrups in the repaired region), flexural cracks first appeared at approximately 1% drift. At 3.7% drift, the cracks in the repaired zone significantly widened, the concrete cover started to spall off, followed by buckling of a couple of longitudinal reinforcements. Finally, at 5.4% drift, a fracture developed at one of the buckled reinforcements at the side with thinner shell, as shown in Figure 7. The test was then stopped.

At the initial loading stage, the response of Unit 2 (specimen with stirrups in the repaired region) was similar to Unit 1. The first sign of concrete crush and diagonal crack happened at 3.7% drift, followed by an extensive plateau in the load-displacement response of the specimen. The concrete cover started to spall off at 5.4% drift, and the diagonal crack got wider but was still narrower than the ones in Unit 1. Eventually, the specimen fractured at 9% drift, as shown in Figure 8.

Flexural cracks on Unit 3 (Specimen without repair) first appeared at approximately 1.8% drift. At the second cycle of 1.8% drift, the cracks significantly widened, the concrete cover started to spall off, followed by buckling of a couple of longitudinal reinforcements. Finally, at 5.4% drift, all the longitudinal reinforcements buckled, as shown in Figure 9, and then the test was stopped.

4 Results

In order to evaluate the lateral strength and ductility of the repaired columns, the recorded force, displacement, and curvature data were used to generate force-displacement, moment-displacement, and curvature distributions along the height of the column, and calculate energy dissipation, damping ratio, and stiffness.

Figure 11 shows the force-displacement and moment-displacement plots, where the shape of hysteretic loops indicates an approximately linear response at the initial loading stage for all specimens. The load capacity of Units 1 and 2 decreased during the test, due to concrete crush and longitudinal reinforcements buckling; however, the specimens were able to sustain 80% of the maximum horizontal force corresponding to a peak displacement at 5.5% drift. After the rebar rupture, the lateral strength of Units 1 and 2 decreased up to 50% and 40%, respectively. The load capacity of Unit 3 decreased dramatically during the test, due to longitudinal reinforcements buckling at 3.7% drift.

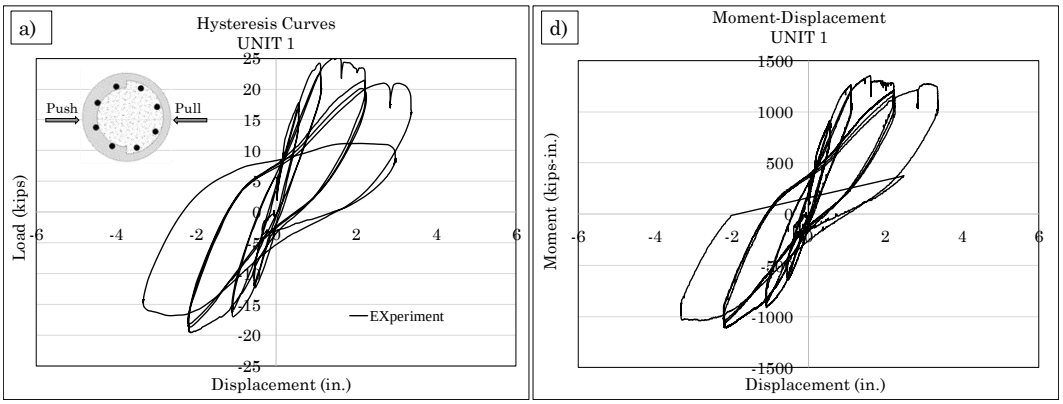

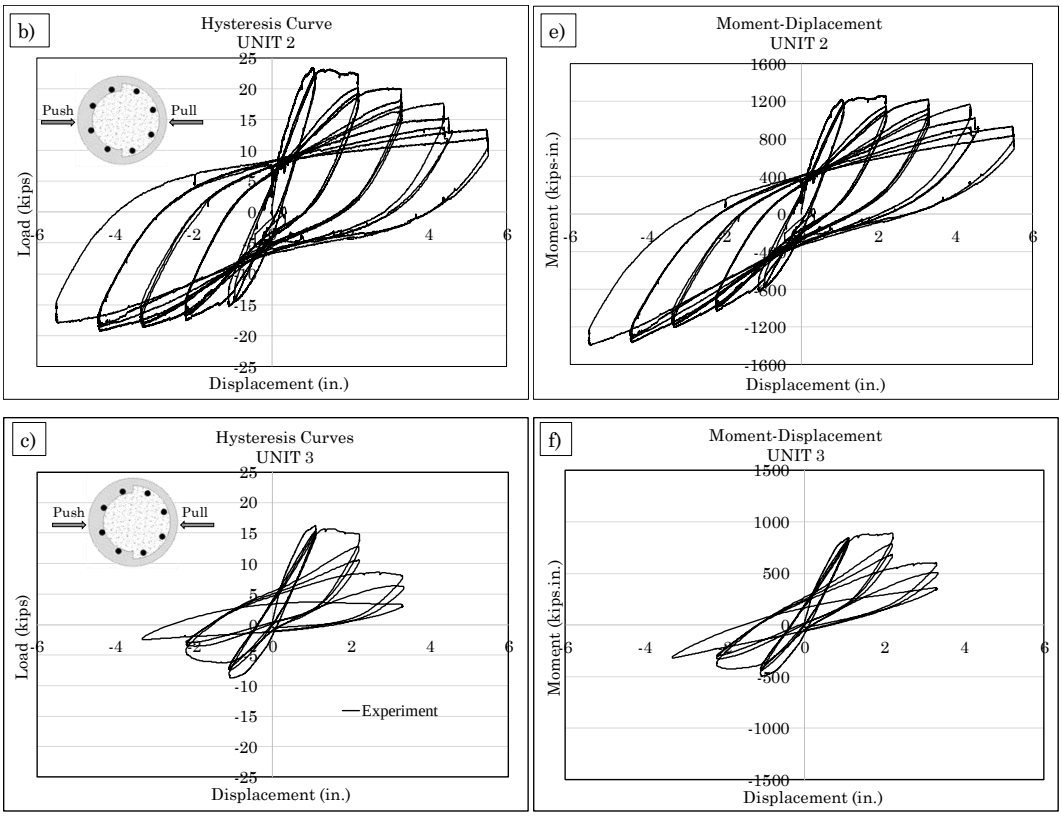

Figure 11. Force-displacement hysteretic responses of a) Unit 1, b) Unit 2, c) Unit 3; Moment-displacement hysteretic responses of d) Unit 1, e) Unit 2, f) Unit 3.

The experimental peak curvatures measured within the repaired region and 4 in. (10 cm) above that are shown in Figure 12.

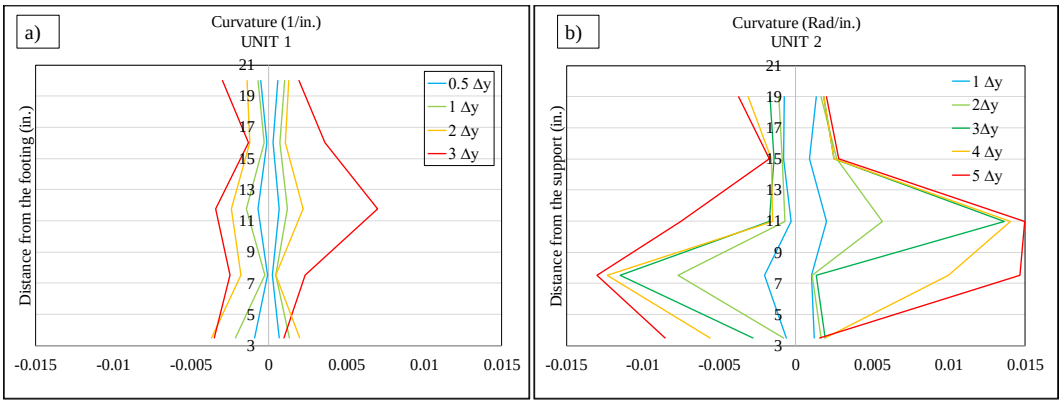

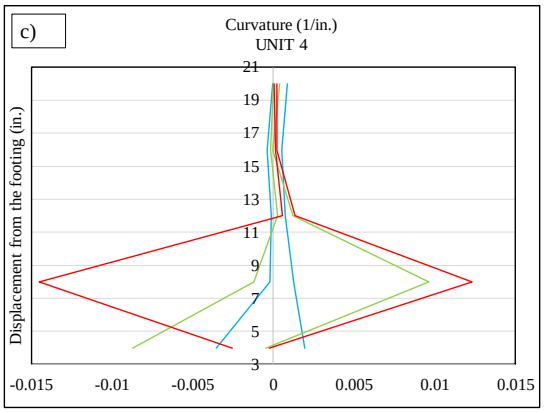

Figure 12. Curvatures measured along the columns a) Unit 1, b) Unit 2, and c) Unit 3.

The stiffness of the test specimens, defined as the slope of the load-displacement curves, during each cycle of each displacement ductility ratio are compared in Figure 13a. Figure 13b shows stiffness degradation plotted against the applied cycle number. Unit 1 exhibited approximately the same stiffness degradation as Unit 2. However, unit 1 failed much earlier than unit 2.

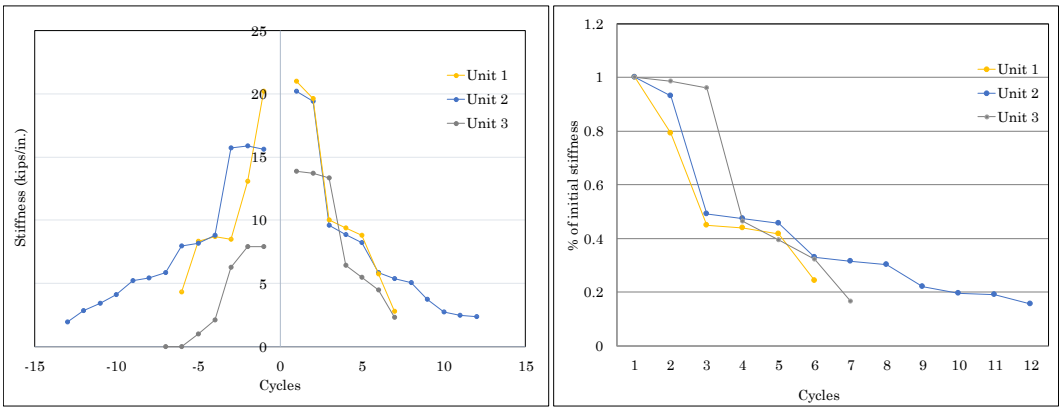

Figure 13. a) Stiffness curves; b) Stiffness degradation curves.

Figure 14 shows dissipated energy per each cycle and the cumulative dissipated energy for each specimen, calculated based on the enclosed area within the hysteresis loops. Results indicate that adding transverse steel reinforcement improves the energy dissipation of the column.

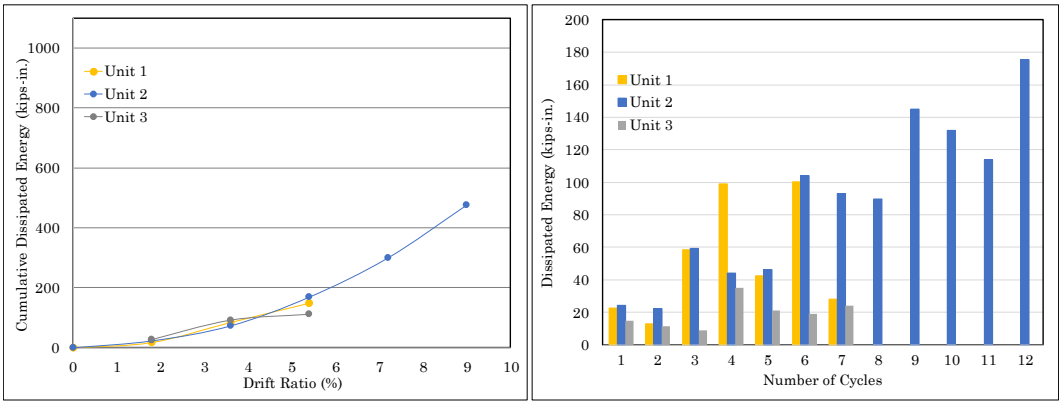

Figure 14. Energy dissipation vs. number of cycles.

The damping ratio (ξ) for each drift ratio was calculated using the following formula:

$$\xi = \frac{E_h}{4\pi E_c}$$

Where E_h is the hysteretic dissipated energy and E_c is the elastic energy calculated based on the maximum displacement and peak load in each cycle [36]. Results presented in Figure 15 shows a higher damping ratio for Unit 2, which could be attributed to the micro-cracks in the concrete core and the yielding of the concrete core's ties.

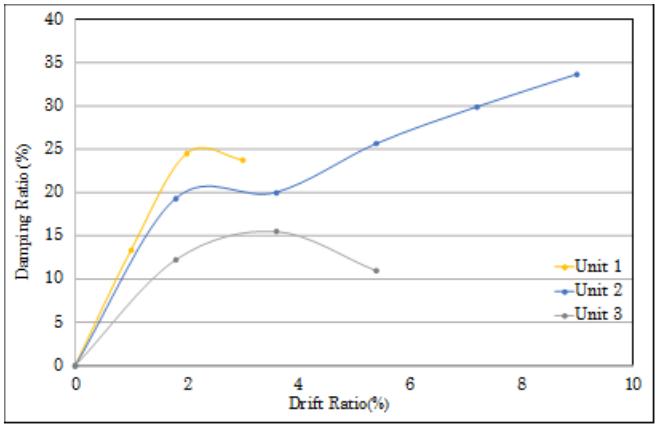

Figure 15. Damping ratios vs. drift ratio.

5 Conclusion

The performance of the proposed retrofit method through experimental and numerical studies has been investigated. A total of three 1/4-scale columns were cast, and artificial damages were created in them. One column was considered as the baseline, and two of the columns were repaired using UHPC. Mechanical performance of the repaired columns was compared with the baseline. The obtained experimental results reveal that the UHPC shell increases the strength of the damaged elements, without increasing its size.

The repair scheme using the UHPC is rather efficient regarding lateral strength, deformation, energy dissipation capacity, and stiffness degradation. Furthermore, lack of any delamination across the circumferential shell shows the effectiveness of the surface preparation, which is a prerequisite for a successful restoration. No sudden cover spalling was observed at repaired areas. UHPC shell transforms the sudden cover spalling to a gradual mechanism. However, it does not prevent bar buckling. This enhancement is due to the ability of the fibers to limit the progression of cracks in the concrete, thereby resulting in greater material integrity at large strains.

Experimental findings indicate that a slight increase of lateral reinforcement significantly improves the cyclic behavior of the specimen, energy dissipation capacity, deformability, and ductility.

This is part of an ongoing research on the application of UHPC in the repair of bridge columns. Flowability, early strength gain, low permeability, and durability of UHPC make it a suitable choice as a repair material. However, to evaluate the efficiency of the repair procedures and fully understand the mechanical behavior of the repaired structure, further numerical and experimental studies are required.

6 Acknowledgement

The research study, results of which are reported in this paper, was partially sponsored by Accelerated Bridge Construction University Transportation Center (ABC-UTC) at Florida International University with the Iowa State University and the University of Nevada-Reno as partners. ABC-UTC is a Tier 1 UTC funded by U.S. DOT. The authors would like to acknowledge and thank the sponsors for their support. Opinions and conclusions expressed in this paper are of the authors and do not necessarily represent those of sponsors. The authors are also thankful to Lafarge, for providing the Ductal® (UHPC) material.

7 References

[1] M. F. Petrou, D. Parler, K. A. Harries, and D. C. Rizos, "Strengthening of Reinforced Concrete Bridge Decks Using Carbon Fiber-Reinforced Polymer Composite Materials," *J. Bridg. Eng.*, vol. 13, no. 5, pp. 455–467, 2008.

[2] K. K. Antoniades, T. N. Salonikios, and A. J. Kappos, "Evaluation of hysteretic response and strength of repaired R/C walls strengthened with FRPs," *Eng. Struct.*, vol. 29, no. 9, pp. 2158–2171, 2007.

[3] S. F. Jiang, X. Zeng, S. Shen, and X. Xu, "Experimental studies on the seismic behavior of earthquake-damaged circular bridge columns repaired by using combination of near-surface-mounted BFRP bars with external BFRP sheets jacketing," *Eng. Struct.*, vol. 106, pp. 317–331, 2016.

[4] H. Sezen, M. Asce, and E. A. Miller, "Experimental Evaluation of Axial Behavior of Strengthened Circular Reinforced-Concrete Columns."

[5] A. Griezic, W. D. Cook, and D. Mitchell, "Seismic Behavior and Retrofit of Outrigger Beam-Column Frames," *J. Bridg. Eng.*, vol. 6, no. 5, pp. 340–348, Oct. 2001.

[6] N. K. Shattarat and D. I. McLean, "Seismic Behavior and Retrofit of Outrigger Knee Joints," *J. Bridg. Eng.*, vol. 12, no. 5, pp. 591–599, Sep. 2007.

[7] E. S. Júlio, F. Branco, and V. D. Silva, "Structural rehabilitation of columns with reinforced concrete jacketing," *Prog. Struct. Eng. Mater.*, vol. 5, no. 1, pp. 29–37, 2003.

[8] E. Denarié, J. S.-R. W. on Bonded, and undefined 2004, "Structural behaviour of bonded concrete overlays," *infoscience.epfl.ch*.

[9] A. Lampropoulos, … O. T.-A. M., and undefined 2012, "Biaxial Stress due to Shrinkage in Concrete Jackets of Strengthened Columns.," *search.ebscohost.com*.

[10] G. Ruano, F. Isla, D. Sfer, and B. Luccioni, "Numerical modeling of reinforced concrete beams repaired and strengthened with SFRC," *Eng. Struct.*, vol. 86, pp. 168–181, 2015.

[11] H. Rodrigues, A. Furtado, A. Arêde, N. Vila-Pouca, and H. Varum, "Experimental study of repaired RC columns subjected to uniaxial and biaxial horizontal loading and variable axial load with longitudinal reinforcement welded steel bars solutions," *Eng. Struct.*, vol. 155, pp. 371–386, 2018.

[12] H. K. Cheong and N. Macalevey, "Experimental Behavior of Jacketed Reinforced Concrete Beams," *J. Struct. Eng.*, vol. 629, 2000.

[13] K. Habel, E. Denarié, and E. Brühwiler, "Structural Response of Elements Combining

Ultrahigh-Performance Fiber-Reinforced Concretes and Reinforced Concrete," *J. Struct. Eng.*, vol. 132, no. 11, pp. 1793–1800, 2006.

[14] R. Abbasnia, P. Godossi, and J. Ahmadi, "Prediction of restrained shrinkage based on restraint factors in patching repair mortar," *Cem. Concr. Res.*, vol. 35, no. 10, pp. 1909–1913, 2005.

[15] K. Wille, A. E. Naaman, and J. P.-M. Gustavo, "Ultra-High Performance Concrete with Compressive Strength Exceeding 150 MPa (22 ksi): A Simpler Way," *ACI Mater. J.*, vol. 108, no. 1, 2011.

[16] H. Russel, G and B. a. Graybeal, "Ultra-High Performance Concrete : A State-of-the-Art Report for the Bridge Community," *No. FHWA-HRT-13-060*, no. June, p. 171, 2013.

[17] A. M. T. Hassan, S. W. Jones, and G. H. Mahmud, "Experimental test methods to determine the uniaxial tensile and compressive behaviour of ultra high performance fibre reinforced concrete (UHPFRC)," *Constr. Build. Mater.*, vol. 37, pp. 874–882, 2012.

[18] B. Graybeal, "Ultra-high performance concrete," *No. FHWA-HRT-11-038*, 2011.

[19] B. A. Graybeal, "Material property characterization of ultra-high performance concrete," *No. FHWA-HRT-06-103*, 2006.

[20] M. Shafieifar, M. Farzad, and A. Azizinamini, "Experimental and numerical study on mechanical properties of Ultra High Performance Concrete (UHPC)," *Constr. Build. Mater.*, vol. 156, pp. 402–411, 2017.

[21] M. Farzad, A. Mohammadi, M. Shafieifar, H. Pham, and A. Azizinamini, "Development of Innovative Bridge Systems Utilizing Steel-Concrete-Steel Sandwich System," in *Transportation Research Record: Journal of the Transportation Research Board*.

[22] M. Farzad, D. Garber, A. Azizinamini, and K. Lau, "Corrosion Macrocell Development in Reinforced Concrete with Repair UHPC," in *Nace International*, 2018.

[23] M. Shafieifar, M. Farzad, and A. Azizinamini, "A comparison of existing analytical methods to predict the flexural capacity of Ultra High Performance Concrete (UHPC) beams," *Constr. Build. Mater.*, vol. 172, pp. 10–18, 2018.

[24] F. A. Farhat, D. Nicolaides, A. Kanellopoulos, and B. L. Karihaloo, "High performance fibre-reinforced cementitious composite (CARDIFRC)–Performance and application to retrofitting," *Eng. Fract. Mech.*, vol. 74, no. 1, pp. 151–167, 2007.

[25] A. P. Lampropoulos, A. P. Spyridon, O. T. Tsioulou, and E. D. Stephanos, "Strengthening of reinforced concrete beams using ultra high performance fibre reinforced concrete (UHPFRC)," *Eng. Struct.*, vol. 106, pp. 370–384, 2016.

[26] C. Beschi, A. Meda, and P. Riva, "Column and Joint Retrofitting with High Performance Fiber Reinforced Concrete Jacketing," *J. Earthq. Eng.*, vol. 15, no. 7, pp. 989–1014, 2011.

[27] M. Farzad, M. Shafieifar, and A. Azizinamini, "Accelerated Retrofitting of Bridge Elements Subjected to Predominantly Axial Load Using UHPC Shell," 2018.

[28] M. Shafieifar, M. Farzad, and A. Azizinamini, "New Connection Detail to Connect Precast Column to Cap Beam Using UHPC in ABC Applications," *Transp. Res. Board 97th Annu. Meet. Res. Board*, no. 18-04892, 2018.

[29] S.-T. Kang and J.-K. Kim, "The relation between fiber orientation and tensile behavior in an Ultra High Performance Fiber Reinforced Cementitious Composites (UHPFRCC)," *Cem. Concr. Res.*, vol. 41, no. 10, pp. 1001–1041, 2011.

[30] M.-A. Dagenais, B. Massicotte, and B.-P. Guillaume, "Seismic Retrofitting of Rectangular Bridge Piers with Deficient Lap Splices Using Ultrahigh-Performance Fiber-Reinforced Concrete," *J. Bridg. Eng.*, vol. 23, no. 2, 2017.

[31] L. Aashto, "Bridge design specifications," 1998.

[32] P. T.-P. Journal and undefined 2003, "Interim Guidelines for the Use of Self-Consolidating Concrete in PCI Member Plants," *imcyc.com*.

[33] ASTM and C43, "143, Standard Test Method for Slump of Hydraulic Cement Concrete," *ASTM Int.*, 2003.

[34] ASTM and C39, "39, Standard test method for compressive strength of cylindrical concrete specimens," *ASTM Int.*, 2001.

[35] ASTM and C, "1018:'Standard Test Method for Flexural Toughness and First-Crack Strength of Fiber-Reinforced Concrete (Using Beam With Third-Point Loading)," *ASTM Int.*, 1997.

[36] "Zohrevand, Pedram, and Amir Mirmiran. 'Effect of column parameters on cyclic behavior of ultra-high-performance concrete-filled fiber-reinforced polymer tubes.' ACI Structural Journal 110, no. 5 (2013): 823."